

TIMELIKE GEODESICS AROUND A CHARGED SPHERICALLY SYMMETRIC DILATON BLACK HOLE

C. Blaga

*Faculty of Mathematics and Computer Science, Babeş-Bolyai University Cluj-Napoca
Kogălniceanu Street 1, Cluj-Napoca, Romania*

E-mail: *cpblaga@math.ubbcluj.ro*

(Received: December 29, 2014; Accepted: March 3, 2015)

SUMMARY: In this paper we study the timelike geodesics around a spherically symmetric charged dilaton black hole. The trajectories around the black hole are classified using the effective potential of a free test particle. This qualitative approach enables us to determine the type of orbit described by test particle without solving the equations of motion, if the parameters of the black hole and the particle are known. The connections between these parameters and the type of orbit described by the particle are obtained. To visualize the orbits we solve numerically the equation of motion for different values of parameters involved in our analysis. The effective potential of a free test particle looks different for a non-extremal and an extremal black hole, therefore we have examined separately these two types of black holes.

Key words. black hole physics – gravitation – relativistic processes

1. INTRODUCTION

In classical general relativity the geometry of the spacetime near a charged black hole is described by Reissner-Nordström metric. In the low-energy string theory, the solution for a static charged black hole was obtained by Gibbons and Maeda (1988) and three years later, independently, by Garfinkle, Horowitz and Strominger (1991). Thus the static spherically symmetric charged dilaton black hole is known as Gibbons–Maeda–Garfinkle–Horowitz–Strominger (GMGHS) black hole.

In 1993, using a Harrison-like transformation (Harrison 1968) to the Schwarzschild solution, Horowitz (1993) derived a metric that fulfills Einstein-Maxwell field equations. For a massless dilaton the solution found by Horowitz corresponds to a GMGHS black hole.

The line element of the metric is:

$$ds^2 = - \left(1 - \frac{2M}{r} \right) dt^2 + \frac{1}{\left(1 - \frac{2M}{r} \right)} dr^2 + r \left(r - \frac{Q^2}{M} \right) (d\theta^2 + \sin^2 \theta d\varphi^2), \quad (1)$$

where Q is related to electrical charge of a black hole and M to its mass. If $Q^2 < 2M^2$ the singularity is inside the event horizon. If $Q^2 = 2M^2$, the area of the event's horizon shrinks to zero. This case is known as *the extremal limit*.

The region inside the event's horizon of a black hole cannot be seen by an external observer. All the information concerning the black hole are derived studying the behaviour of matter and light in its exterior. A free test particle moves on a timelike geodesics and a photon on a null geodesics. This is the reason why if we want to describe the motion in the vicinity of a black hole we have to solve the geodesic equations.

In classical general relativity as well as in string theory, geodesics of black holes are studied extensively. The critical parameters for photon and timelike geodesics for Kerr black holes and Reissner-Nordström black holes have been found from conditions for multiple roots of corresponding polynomials by Zakharov (1994, 2014) and Zakharov et. al. (2005a,b, 2014). The null geodesics of static charged black holes in heterotic string theory were analysed by Fernando (2012). The circular null and timelike geodesics for a non-extremal and extremal GMGHS black hole were investigated by Pradhan (2012). The exact solutions of timelike geodesics of an extremal GMGHS black hole were derived in Blaga and Blaga (1998). The existence and stability of circular orbits for the timelike geodesics of a GMGHS black hole were examined in Blaga (2013). A quantitative analysis of the timelike geodesics of a charged black hole in heterotic string theory was done by Olivares and Villanueva (2013), article in which the authors obtained the solution of geodesic equations in terms of elliptic \wp -Weierstrass function.

Our goal is to classify the orbits of free test particles in the vicinity of a spherically symmetric dilaton black hole using the effective potential. This approach enables us to identify the type of orbit described by a particle around a GMGHS black hole without solving the equations of motion. The type of the orbit described by a free test particles around a given GMGHS black hole depends on its angular momentum, energy and initial position. The qualitative results are accompanied by plots of possible orbits described by free test particles around different GMGHS, obtained by numerical integration of the equations of motion. The initial condition for a given type of black hole was chosen using the knowledge about peculiarities of the effective potential.

The paper is organized as follows: in Section 2 we derive the geodesic equations from the Lagrangian corresponding to metric Eq. (1). In Section 3 we emphasize some properties of the effective potential of a free test particle for both a non-extremal and extremal GMGHS. In Section 4 we classify the possible trajectories around a GMGHS black hole with $b \in [0, 2)$, respectively $b = 2$ and plot the numerical solution of the geodesic equations for different values of the parameters involved in our analysis. The conclusion are given in the last section.

2. GEODESIC EQUATIONS

We can derive the geodesic equations by directly computing the Christoffel coefficients for the given metric or by using Hamilton-Jacobi theory (see for example Blaga and Blaga 1998) or by writing the Euler-Lagrange equations (see Fernando 2012). We follow here the later approach described by Chandrasekhar (1983). The Lagrangian for the metric Eq. (1) is:

$$2\mathcal{L} = - \left(1 - \frac{2M}{r}\right) \dot{t}^2 + \left(1 - \frac{2M}{r}\right)^{-1} \dot{r}^2$$

$$+ r \left(r - \frac{Q^2}{M}\right) \left(\dot{\theta}^2 + \sin^2 \theta \dot{\varphi}^2\right), \quad (2)$$

where the dot means the differentiation with respect to τ - the affine parameter along the geodesic. This parameter is chosen so that $2\mathcal{L} = -1$ on a timelike geodesic, $2\mathcal{L} = 0$ on a null geodesic and $2\mathcal{L} = 1$ on a space-like geodesic.

The coordinates t and φ are cyclic. Therefore the motion has two first integrals derived from the Euler-Lagrange for time and latitude as follows. From the Euler-Lagrange equation for t we get:

$$\left(1 - \frac{2M}{r}\right) \dot{t} = E, \quad (3)$$

known as the energy integral. The real constant E is the total energy of the particle. The second integral of motion is obtained from the Euler-Lagrange for φ :

$$2r \left(r - \frac{Q^2}{M}\right) \sin^2 \theta \dot{\varphi} = \text{constant}, \quad (4)$$

known as the integral of angular momentum.

From the Euler-Lagrange equation for θ we get:

$$\frac{d}{d\tau} \left[r \left(r - \frac{Q^2}{M}\right) \dot{\theta} \right] = r \left(r - \frac{Q^2}{M}\right) \sin \theta \cos \theta \cdot \dot{\varphi}^2. \quad (5)$$

Considering $\theta = \pi/2$ when $\dot{\theta} = 0$, then $\ddot{\theta} = 0$ and $\theta = \pi/2$ on geodesic. This means that the motion is confined in a plane as in the Schwarzschild spacetime or in Newtonian gravitational field.

If $\theta = \pi/2$ during the motion the angular momentum integral Eq. (4) becomes:

$$r \left(r - \frac{Q^2}{M}\right) \dot{\varphi} = L, \quad (6)$$

where the real constant L is the angular momentum about an axis normal to the plane in which the motion took place.

The Euler-Lagrange equation corresponding to the radial coordinate is complicated. Therefore, we replace it with a relation derived from the constancy of the Lagrangian. If we substitute in Eq. (2) \dot{t} from Eq. (3), $\dot{\varphi}$ from Eq. (6) and $\dot{\theta}$ from Eq. (5), after some algebra we get:

$$\left(\frac{dr}{d\tau}\right)^2 + \left(1 - \frac{2M}{r}\right) \left(\frac{L^2}{r \left(r - \frac{Q^2}{M}\right)} - \epsilon\right) = E^2, \quad (7)$$

where $\epsilon = -1$ for timelike geodesics, $\epsilon = 0$ for null geodesics and $\epsilon = +1$ for space-like geodesics.

2.1. Radial timelike geodesics

The angular momentum of a free test particle moving on a radial timelike geodesics is zero. Therefore Eq. (7) becomes:

$$\left(\frac{dr}{d\tau}\right)^2 + \left(1 - \frac{2M}{r}\right) = E^2. \quad (8)$$

If we want to study the motion of a test particle which describes a radial timelike geodesic we have to consider Eq. (8) for radial coordinate r and the Euler-Lagrange equation for time coordinate t :

$$\frac{dt}{d\tau} = \frac{E}{\left(1 - \frac{2M}{r}\right)}, \quad (9)$$

where τ is the proper time. These two equations are identical with the equations of radial timelike geodesics in the Schwarzschild spacetime (Chandrasekhar 1983). Therefore, the motion of free test particles on radial geodesics in the vicinity of these two kind of black holes will have the same properties. It is well known that an observer stationed at a large distance from a Schwarzschild black hole finds that a free falling test particle approaches to events horizon but can never cross it, because the test particle needs an infinite time t to reach the horizon even though it crosses the horizon in a finite proper time τ . This property is valid for a free falling particle on a radial timelike geodesic of GMGHS black holes, too.

3. EFFECTIVE POTENTIAL FOR TIMELIKE GEODESICS

If we compare Eq. (7) with $\dot{r}^2 + V_{\text{eff}} = E^2$ we get the effective potential:

$$V_{\text{eff}} = \left(1 - \frac{2M}{r}\right) \left(\frac{L^2}{r\left(r - \frac{Q^2}{M}\right)} - \epsilon\right), \quad (10)$$

which depends on radial coordinate r , the parameters related to the electrical charge and mass of the black hole, the type of the geodesics and the angular momentum of the particle.

For timelike geodesics $\epsilon = -1$ and Eq. (10) becomes

$$V_{\text{eff}} = \left(1 - \frac{2M}{r}\right) \left(\frac{L^2}{r\left(r - \frac{Q^2}{M}\right)} + 1\right). \quad (11)$$

In order to lower the number of parameters from the effective potential we denote $u = r/M$, $a = (L/M)^2$, $b = (Q/M)^2$ and the Eq. (11) becomes:

$$V_{\text{eff}} = \left(1 - \frac{2}{u}\right) \left(\frac{a}{u(u-b)} + 1\right). \quad (12)$$

The quantity $q = Q/M$ is the specific electrical charge and we observe that $b = q^2$. In this paper we have assumed that $Q^2 \leq M^2$ hence $b \in [0, 2]$, where $b = 0$ is for a Schwarzschild black hole and $b = 2$ for an extremal GMGHS black hole. The parameter a equals $(L/M)^2$, therefore in our study it will be positive or zero. In the new variable u , the events horizon corresponds to $u = 2$ and the region outside the horizon will be given by $u > 2$.

3.1. Effective potential for $b \in [0, 2)$

The effective potential Eq. (12) was studied in Blaga (2013). The qualitative analysis of V_{eff} revealed that for $b \in [0, 2)$, the function is positive for $u \in [2, +\infty)$, it is zero on the events horizon $u = 2$ and approaches 1 as u approaches $+\infty$ (see Fig. 1). If a is greater than a value depending on b (see Blaga 2013), the potential has two local extreme points outside the events horizon, the local maximum point of V_{eff} being closest to the horizon. For a given b , if there is a local maximum point outside the horizon, the maximum value of the potential increases with a .

In Fig. 1 we have plotted the effective potential against $u = r/M$ for $b = 1$ and three values of a . The first value $a = 8.41054$ is the lowest value of a for which V_{eff} admits extreme points outside the horizon for $b = 1$ (see Blaga 2013). The second value $a = 12$ is the lowest value of a for which the effective potential admits extreme points outside the horizon in the case of a Schwarzschild black hole $b = 0$ (see Chandrasekhar 1983).

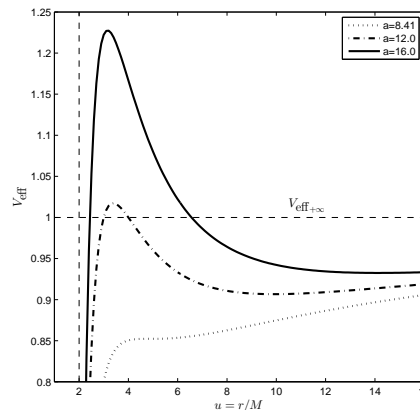


Fig. 1. Effective potential for $b = 1$ and $a \in \{8.41, 12, 16\}$. The dashed lines are for the vertical $u = 2$ - events horizon and horizontal $V_{\text{eff}} = 1$ - the limit of the potential as $u \rightarrow +\infty$.

If we choose another value for $b \in [0, 2)$ different from 1, the graph of the effective potential is similar, but for a given value of a , if the potential admits two extreme points outside the events horizon, the maximum value of the potential increases with b (see Blaga 2013).

3.2. Effective potential for $b = 2$

For a test particle moving around an extremal GMGHS black hole $b = 2$ the effective potential is:

$$V_{\text{eff}}(u) = \frac{u^2 - 2u + a}{u^2}, \quad (13)$$

a function which is not defined in $u = 0$, approaches infinity as u approaches zero and 1 as u approaches infinity (see Fig. 2). In this case the effective potential admits only a local minimum point in $u = a$. This point is outside the events horizon if and only if $a \geq 2$. The minimum value of the effective potential increases with a , it approaches 1 from below as a approaches $+\infty$. We have plotted the effective potential Eq. (13) for various values of a in Fig. 2.

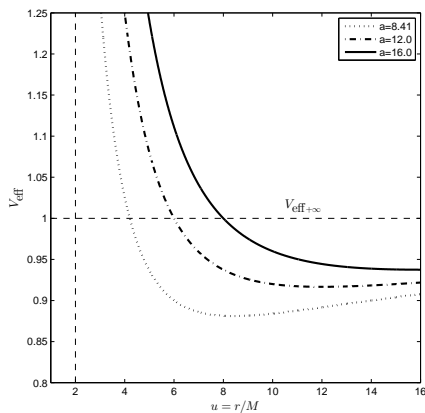


Fig. 2. *Effective potential for $b = 2$ and $a \in \{8.41, 12, 16\}$. The dashed lines are for the vertical $u = 2$ - events horizon and horizontal $V_{\text{eff}} = 1$ - the limit of the potential as $u \rightarrow +\infty$.*

4. TYPES OF TIMELIKE GEODESICS

If we replace $\varepsilon = -1$ in Eq. (7) we get the equation of motion of a free test particle around a spherically symmetric charged black hole. Therefore, the geometry of the orbit described by the test particle depends on its energy.

The motion is possible only if $E^2 - V_{\text{eff}}(u) \geq 0$. The points in which $E^2 = V_{\text{eff}}(u)$ are known as turning points because $dr/dt = 0$ and the direction of motion could be changed there.

4.1. Orbits around a dilaton black hole with $b \in [0, 2)$

In Fig. 3 we have plotted the effective potential for a dilaton black hole with $b = 1$ as an exponent for GMGHS black holes with $b \in [0, 2)$. The parameter $a = 12$. The points A and B represent the maximum, and minimum point of the effective potential respectively. The dashed horizontal lines

are for the maximum value of potential $V_{\text{eff,max}}$, the minimum value $V_{\text{eff,min}}$ and the limit of the potential as u approaches infinity $V_{\text{eff},+\infty}$. The horizontal solid lines represent different energy levels. C , D , F and H denote the intersection points of energy level with the graph of the effective potential. The points in which a test particle crosses the line $u = 2$ are denoted by G and K .

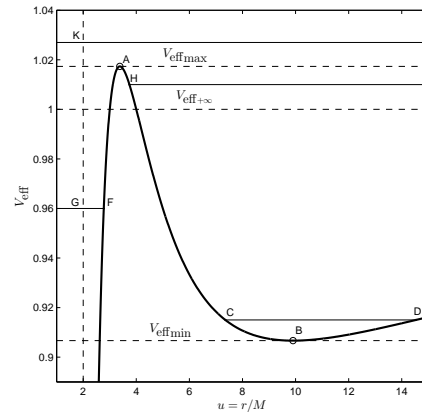


Fig. 3. *Effective potential for $b = 1$ and $a = 12$. Dashed lines are for the extreme values of the effective potential, the limit of the potential as u approaches infinity $V_{\text{eff},+\infty}$ and the vertical $u = 2$. The solid lines are for different energy levels.*

If we consider a free test particle moving around a dilaton black hole with $b \in [0, 2)$ and a greater than the lower value for which the effective potential has extrema outside the events horizon, the graph of the effective potential is similar to the graph in Fig. 3. The reason why we have computed the orbits around a GMGHS black hole with $b = 1$ is to visualize the geometry of possible trajectories around GMGHS black holes with an arbitrary $b \in [0, 2)$. In the following polar plots we have represented the region inside events horizon as a circle filled with black. The orbits were obtained by numerical integration of Eq. (7) and Eq. (6) using MATLAB.

If the motion of a free test particle around a dilaton black hole is possible then, depending on the total energy of the test particle and its initial position u_0 , we can find the following qualitative motions:

Case 1: if $E^2 > V_{\text{eff,max}}$ then the test particle approaches the black hole, crosses the events horizon and ends into the singularity. The particle is gravitationally captured.

In Fig. 4 we have represented a gravitational capture. The free test particle is moving with the total energy corresponding to the highest energy from Fig. 3, crosses the events horizon in K and end into the singularity.

Case 2: if $E^2 \in (1, V_{\text{eff,max}})$, $u_0 > u(A)$ and the motion is possible the test particle approaches the black hole until its squared energy equals the potential and then goes back to infinity (see Fig. 5). We say that the particle is scattered hyperbolically or it has an hyperbolic motion.

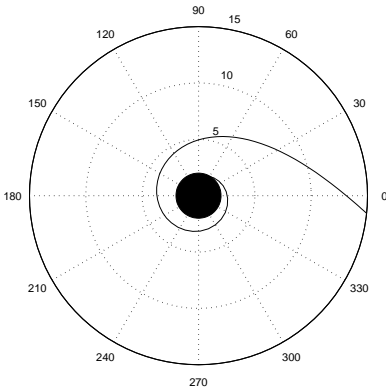


Fig. 4. *Gravitational capture.* Here $a = 12$, $b = 1$, $E^2 = 1.03$ and $u_0 = 15.0$.

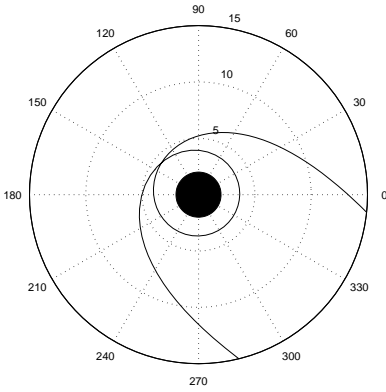


Fig. 5. *Hyperbolic scattering.* Here $a = 12$, $b = 1$, $E^2 = 1.01$ and $u_0 = 15.0$.

In Fig. 5 we have represented the orbit of a test particle with an energy equal to the energy from the second energy level from Fig. 3. In H the test particle change its direction of motion and turns back to large distances from the black hole.

Case 3: if $E^2 = V_{\text{eff,max}}$ and $u_0 = u(A)$ then the test particle describes a circular orbit around the black hole (see Fig. 6). Since A is a local maximum point for effective potential the circular orbit is unstable.

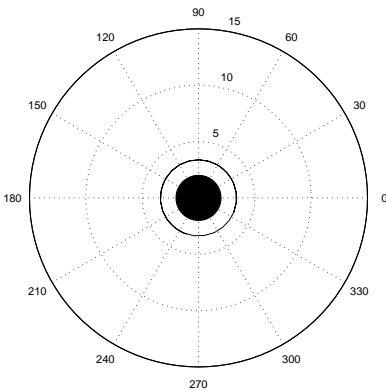


Fig. 6. *Unstable circular motion.* Here $a = 12$, $b = 1$, $E^2 = 1.073$ and $u_0 = 3.381$.

Case 4: if $E^2 = V_{\text{eff,max}}$, $u_0 > u(A)$ and the motion is possible, the particle escapes to infinity. We say that it is moving on an outer marginal orbit (see Fig. 7). If $E^2 = V_{\text{eff,max}}$ and $u_0 < u(A)$, the particle ends into the singularity and we say that it describes an inner marginal orbit (see Fig. 8).

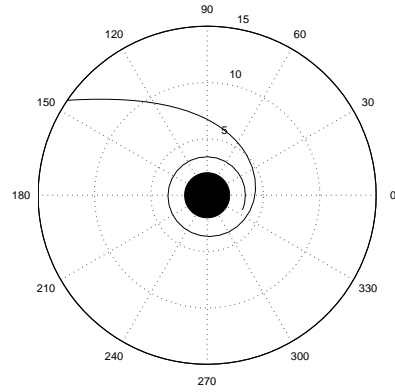


Fig. 7. *Outer marginal orbit.* Here $a = 12$, $b = 1$, $E^2 = 1.073$, $u_0 = 3.39$.

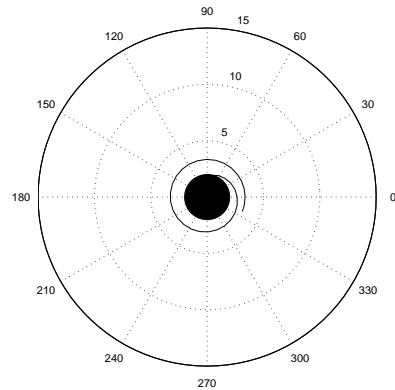


Fig. 8. *Inner marginal orbit.* Here $a = 12$, $b = 1$, $E^2 = 1.073$, $u_0 = 3.37$.

Case 5: if $E^2 < V_{\text{eff,max}}$, $u_0 < u(A)$ and motion is possible then the test particle moves toward the singularity crossing the horizon in F (see Fig. 9). Motion is trapped near the horizon.

Case 6: if $E^2 \in (V_{\text{eff,min}}, \min(1, V_{\text{eff,max}}))$, $u_0 > u(A)$ and motion is possible then the test particle moves toward and backward from the black hole. C and D are the points where the test particle changes its direction of motion. The orbit is bounded and the motion is restricted in the annular region placed between the circles with radius $u(C)$ and $u(D)$, respectively.

In Fig. 10 we have plotted the orbit of a free test particle with energy corresponding to the lowest energy level from Fig. 3. The dashed lines are for circles with radius $u = u(C)$ - the lower limit of the distance between the test particle and the singularity ($u = 0$), and $u = u(D)$ - the upper limit of the same distance, respectively.

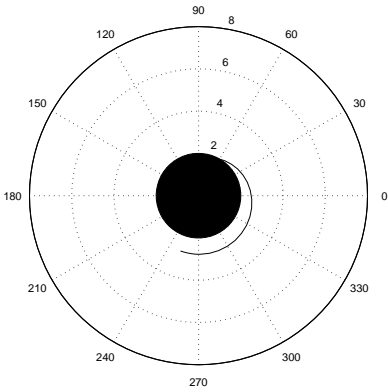


Fig. 9. *Motion trapped near the horizon.* Here $a = 12$, $b = 1$, $E^2 = 0.96$, $u_0 = 2.75$.

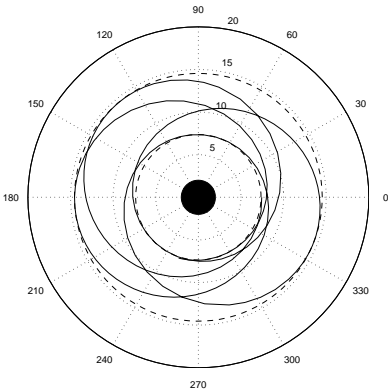


Fig. 10. *Bounded orbit.* Here $a = 12$, $b = 1$, $E^2 = 0.915$, $u_0 = 7.5$, $u(C) = 7.355$, $u(D) = 14.53$.

Case 7: if $E^2 = V_{\text{effmin}}$ and $u_0 = u(B)$ the test particle describes a stable circular orbit, because B locates the minimum point of effective potential (see Fig. 11).

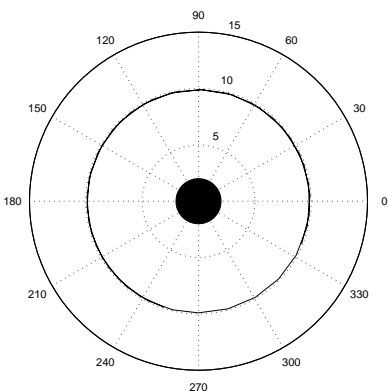


Fig. 11. *Stable circular orbit.* Here $a = 12$, $b = 1$, $E^2 = 0.907$, $u_0 = 9.9$.

The unstable and stable circular orbits are in fact specially bounded orbits with $u = u(A)$ and $u = u(B)$, respectively.

We notice that the type of trajectories enumerated in this section are qualitatively similar to the trajectories found in a Schwarzschild spacetime (see Frolov and Zelnikov 2011). This fact was expected because a Schwarzschild black hole is a GMGHS black hole with $b = 0$. The difference between the orbits around a Schwarzschild black hole and a GMGHS dilaton black hole with $b \in (0, 2)$ appears in dynamical parameters of motion. For example, for a given a the test particle needs a higher energy to be gravitationally captured because the maximum value of the effective potential increases with b .

4.2. Trajectories around an extremal GMGHS black hole

In Fig. 12 we have plotted the effective potential for an extremal dilaton black hole for $a = 12$. The horizontal dashed lines are for the minimum value of effective potential and its limit when $u \rightarrow +\infty$. The vertical $u = 2$ plotted with dashed line corresponds to the events horizon. The energy levels are represented with solid lines. The point B is the minimum point of the effective potential, C , D , F and H are the turning points and G the point in which the test particles cross the horizon.

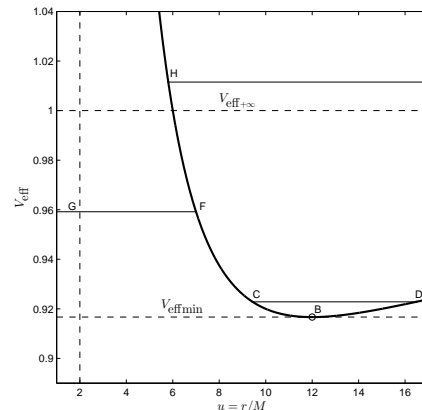


Fig. 12. *Effective potential for $b = 2$.* The dashed lines are for the minimum value of the effective potential, the limit of the potential as u approaches infinity $V_{\text{eff}+\infty}$ and the vertical $u = 2$. The solid lines are for different energy levels.

If we consider a free test particle moving around an extremal dilaton black hole $b = 2$ and $a \geq 2$, then the graph of the effective potential is similar to the plot from Fig. 12. Depending on total energy of the particle and its initial position u_0 a free test particle describes one of the following trajectories:

Case 1: if $E^2 \geq 1$ and $u_0 > u(H)$, where $u(H) > 2$ is a solution of the equation $V_{\text{eff}}(u) = E^2$, the particle will move toward the black hole, arrives at H and goes back to infinity (see Fig. 13). We say that the test particle has a hyperbolic motion, or is hyperbolically scattered. In Fig. 13 we have represented the hyperbolic motion of a test particle with the energy corresponding to the highest energy level from Fig. 12.

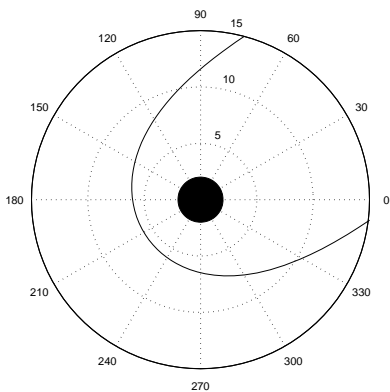


Fig. 13. *Hyperbolic scattering.* Here $a = 12$, $b = 2$, $E^2 = 1.012$, $u_0 = 15.0$.

Case 2: if $E^2 > V_{\text{eff}\min}$ and $u = r/M_0 < u(F)$, where F is a solution of the equation $V_{\text{eff}}(u) = E^2$, the particle falls into the singularity, crossing the horizon in G . In this case the orbit is trapped near the events horizon. In Fig. 14 the total energy of the test particle corresponds to the second energy level from Fig. 12.

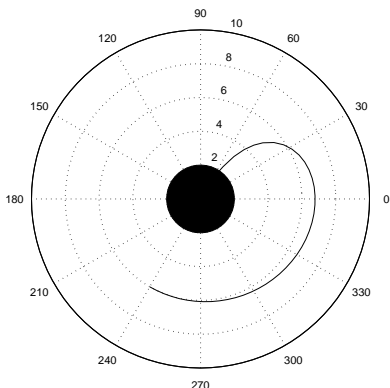


Fig. 14. *Near the horizon trapped motion.* Here $a = 12$, $b = 2$, $E^2 = 0.96$, $u_0 = 6.0$.

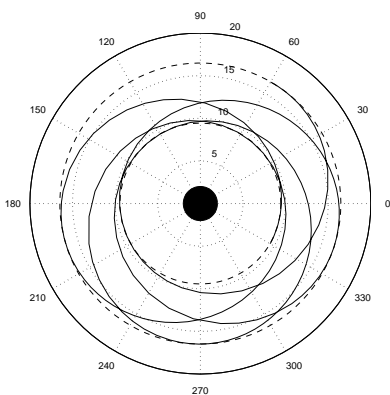


Fig. 15. *Bounded orbit.* Here $a = 12$, $b = 2$, $E^2 = 0.922$, $u_0 = 9.45$. The dashed lines are for the circles $u(C) = 9.43$ and $u(D) = 16.49$.

Case 3: if $E^2 \in (V_{\text{eff}\min}, 1)$ and $u_0 > 2$ the particle moves toward and backward from the black hole. The particle changes its direction of motion in the turning points C and D , respectively (see Fig. 15). In this case the motion is bounded. The radius of the limit circles are the solutions $u > 2$ of the equation $V_{\text{eff}}(u) = E^2$.

Case 4: if $E^2 = V_{\text{eff}\min}$ and $u_0 = u(B)$ the particle describes a stable circular orbit because B is the minimum point of the effective potential (see Fig. 16).

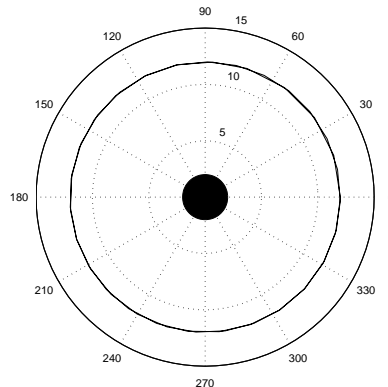


Fig. 16. *Stable circular orbit.* Here $a = 12$, $b = 2$, $E^2 = 0.917$, $u_0 = 12.0$.

We notice that a free test particle is moving near an extremal dilaton black hole on trajectories qualitatively similar to those described in a Newtonian field. This similarity came from the fact that the effective potential Eq. (13) is alike with the effective potential for motion in a Newtonian field (see Frolov and Zelnikov 2011).

5. CONCLUSIONS

In this work we have considered the timelike geodesics of a static, spherically symmetric, charged black hole known as a GMGHS black hole. We have classified the solutions of timelike geodesic equations using the effective potential of a free test particle moving in the vicinity of such a black hole.

The effective potential of a test particle depends on the radial coordinate r , parameter related to the electrical charge Q , mass M of the black hole, and angular momentum of the test particle L . In order to pursue the qualitative analysis of this function we have lowered the number of parameters present in it by introducing a new variable $u = r/M$ and parameters related to the specific electrical charge of the black hole $b = (Q/M)^2$ and the quotient of angular momentum of the particle and mass of black hole $a = (L/M)^2$. We have found that the type of the trajectory described by a free test particle depends on these new parameters and not directly on the electrical charge Q , mass M of the black hole, and angular momentum L of the test particle. Moreover, the ty-

pe of the trajectory depends on the total energy and initial position of the test particle.

We have done the classification of the timelike geodesics of a GMGHS black hole separately for an arbitrary $b \in [0, 2)$ and for $b = 2$, because we have noticed that there are differences between the graphs of the corresponding effective potentials that may be reflected in the geometry of the orbits. Additionally, in order to visualize the trajectories described by test particles, we have determined numerical solutions of geodesic equations for different sets of parameters. The values of the parameters were chosen using the knowledge accumulated during the qualitative study of the effective potential. The numerical solutions were plotted in polar coordinates. Our results are in good agreement with those obtained by Olivares and Villanueva (2013).

Acknowledgements – The author would like to thank the anonymous reviewer for suggestions.

REFERENCES

- Blaga, C. and Blaga, P. A.: 1998, *Serb. Astron. J.*, **158**, 55.
- Blaga, C.: 2013, *Automat. Comp. Appl. Math.*, **22**, 41.
- Chandrasekhar, S.: 1983, *The Mathematical Theory of Black Holes*, Oxford University Press, Oxford.
- Fernando, S.: 2012, *Phys. Rev. D*, **85**, 024033.
- Frolov, V. P. and Zelnikov, A.: 2011, *Introduction to Black Hole Physics*, Oxford University Press, Oxford.
- Garfinkle, T., Horowitz, G. A. and Strominger, A.: 1991, *Phys. Rev. D*, **43**, 3140.
- Gibbons, G. W. and Maeda, K.: 1988, *Nucl. Phys.* **B298**, 741.
- Harrison, B. K.: 1968, *J. Math. Phys.*, **9**, 1744.
- Horowitz, G. A.: 1993, in "Directions in General Relativity", II, eds. B.L. Hu and T.A. Jacobson, Cambridge University Press, Cambridge, 157.
- Olivares, M. and Villanueva, J. R.: 2013, *Eur. Phys. J. C*, **73**, 2659.
- Pradhan, P. P.: 2012, arXiv:1210.0221.
- Zakharov, A. F.: 1994, *Class. and Quantum Gravity*, **11**(4), 1027.
- Zakharov, A. F., De Paolis, F., Ingrosso, G. and Nucita, A. A.: 2005a, *Astron. Astrophys.*, **442**(3), 795.
- Zakharov, A. F., Nucita, A. A., De Paolis, F. and Ingrosso, G.: 2005b *New Astron.*, **10**(6), 479.
- Zakharov, A. F., De Paolis, F., Ingrosso, G. and Nucita, A. A.: 2012, *New Astron. Rev.*, **56**(2), 64.
- Zakharov, A. F.: 2014, *Phys. Rev. D*, **90**(6), 062007.

ВРЕМЕНСКЕ ГЕОДЕЗИЈСКЕ ЛИНИЈЕ ОКО НАЕЛЕКТРИСАНЕ СФЕРНОСИМЕТРИЧНЕ ДИЛАТОНСКЕ ЦРНЕ РУПЕ

C. Blaga

*Faculty of Mathematics and Computer Science, Babeş-Bolyai University Cluj-Napoca
Kogălniceanu Street 1, Cluj-Napoca, Romania*

E-mail: *cpblaga@math.ubbcluj.ro*

УДК 524.882–336

Оригинални научни рад

У овом раду бавимо се временским геодезијским линијама око сферносиметричне наелектрисане дилатонске црне рупе. Трајекторије око црне рупе класификоване су помоћу ефективног потенцијала који делује на слободну пробну честицу. Овај квалитативни приступ омогућава нам да, уколико су параметри црне рупе и пробне честице познати, одредимо тип орбите коју описује чес-

тица без решавања једначина кретања. Добијене су везе између ових параметара и типа орбите честице. У циљу визуализације орбита нумерички су решене и једначине кретања за различите вредности анализираних параметара. Ефективни потенцијал слободне пробне честице изгледа другачије за не-екстремну и екстремну црну рупу, тако да су ова два случаја размотрена посебно.